

# Hybrid Integrator Backstepping Control of Robotic Manipulators Driven by Brushless DC Motors

Chun-Yi Su, *Member, IEEE*, Yury Stepanenko, and Sadik Dost

**Abstract**— In this paper, a hybrid integrator backstepping controller is proposed for robotic manipulators actuated with brushless dc motors in the presence of arbitrary uncertain inertia parameters of the manipulator and the electrical parameters of the actuators. The main features are: 1) the design, requiring at most the joint velocities and stator currents feedback, 2) the semiglobal asymptotic stability of the controller being established in the Lyapunov sense, and 3) suitability of the scheme for multi-joint robots. Simulation results are included to demonstrate the tracking performance.

## I. INTRODUCTION

THE CONTROL of rigid robots including the actuator dynamics has received increasing attention and is a topic of great interest, since actuator dynamics constitute an important part of robot dynamics. This is especially true in both the case of high-velocity movement and highly varying loads [5]. The inclusion of the actuators into the dynamic equations complicates the controller design and its stability analysis since the systems are described by higher order differential equations [18]. Among the developed control methods, much effort is focused on simple brushed dc motors as actuators [2], [4], [6], [16]–[18], because they are relatively easy to control. As indicated in [8], a brushless dc motor (BLDCM) offers several advantages over its brushed counterpart, and is an attractive choice for high-performance servo applications such as the MIT Direct-Drive Arm [1]. However, due to its multi-input nature and the significant nonlinear coupling among the phase currents and the rotor velocity, the control laws developed for brushed dc motors are not applicable. This is the problem which this paper addresses.

The control of the BLDCM has been investigated by many authors including [8], [11], [13], and references therein. However, the study of the control of robots actuated by the BLDCM was relatively recent [3], [7], [11]. In [11], a robust feedback linearizing control was proposed. In [3], [7], by using integrator backstepping techniques [12], robust and adaptive controllers are proposed, respectively. It should be noted however that all those results are suitable only for a single-link manipulator (an inertial load).

The objective of this study is to develop a control scheme for a rigid  $n$ -link manipulator where the joint actuators are

Manuscript received September 4, 1995; revised April 9, 1996. This work was supported by the Natural Science and Engineering Research Council of Canada, the Institute for Robotic and Intelligent Systems (IRIS), and Precarn Associates, Inc.

The authors are with the Department of Mechanical Engineering, University of Victoria, Victoria, B.C., Canada V8W 3P6 (e-mail: csu@sirius.uvic.ca).

Publisher Item Identifier S 1083-4435(96)09043-6.

driven by BLDCM's. Based on the integrator backstepping techniques, a hybrid integrator backstepping controller (i.e., adaptive and robust adaptive) is proposed. The proposed controller has the following features: 1) it does not require joint acceleration feedback; 2) knowledge of the robot or any of the BLDCM uncertain parameters are not required; and 3) a semiglobal asymptotic stability result is obtained in the Lyapunov sense.

The arrangement of this article is as follows: in Section II the robot dynamics including BLDCM is expressed in the form of two cascaded subsystems: the BLDCM subsystem and the manipulator subsystem. In Section III, an embedded control signal is introduced as a synthesized input signal intended for the manipulator subsystem. A control law is then developed to compensate the usually neglected BLDCM subsystem. Asymptotic stability of the adaptive controller is established in the Lyapunov sense. In Section IV, a simplified algorithm is introduced to avoid the calculation of derivative of the regressor matrix. Simulation results are discussed in Section V. Finally, some conclusions are given in Section VI.

## II. DYNAMIC MODEL OF MANIPULATOR WITH BLDCM

Consider an  $n$ -link manipulator with revolute joints driven by general three-phase BLDCM's with voltage input. As in [8] and [13], the dynamic equations of the  $i$ th BLDCM of a robot arm are given by

$$\begin{aligned} R_{si}\ell_{1i} + L_{si}\frac{d\ell_{1i}}{dt} + K_{ei}f_i(\theta_i)\frac{d\theta_i}{dt} &= v_{1i} \\ R_{si}\ell_{2i} + L_{si}\frac{d\ell_{2i}}{dt} + K_{ei}f_i\left(\theta_i - \frac{2\pi}{3}\right)\frac{d\theta_i}{dt} &= v_{2i} \\ R_{si}\ell_{3i} + L_{si}\frac{d\ell_{3i}}{dt} + K_{ei}f_i\left(\theta_i - \frac{4\pi}{3}\right)\frac{d\theta_i}{dt} &= v_{3i}, \\ & i = 1, \dots, n \end{aligned} \quad (1)$$

where

$v_{1i}, v_{2i}, v_{3i}$	a, b, c stator phase voltages, respectively,
$\ell_{1i}, \ell_{2i}, \ell_{3i}$	a, b, c stator phase currents,
$\theta_i$	angular position of rotor,
$R_{si}$	stator resistance,
$L_{si}$	stator inductance,
$K_{ei}$	back EMF constant.

The function  $f_i(\theta_i): R \rightarrow R$  is determined by the motor construction and rotor field distribution and is a continuous

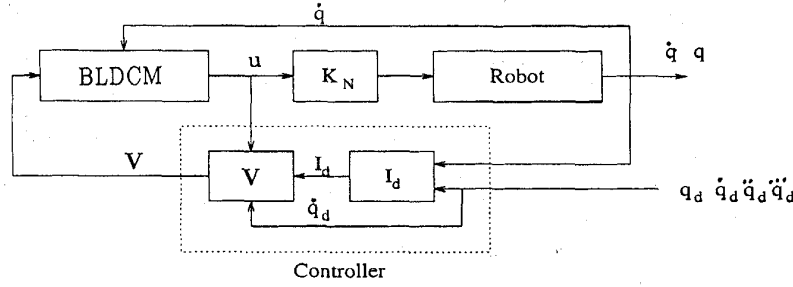


Fig. 1. Control system.

periodic function such that

$$f_i(\theta_i + 2\pi) = f_i(\theta_i), \quad \forall \theta_i \in R. \quad (2)$$

In addition, the sum of three stator phase currents must be zero when the neutral point is floated. That is

$$\sum_{k=1}^3 \ell_{ki} = 0. \quad (3)$$

If we let  $q_i$  denote the  $i$ th joint variable, then

$$\theta_i = N_i q_i, \quad i = 1, \dots, n \quad (4)$$

where  $N_i$  is the gear ratio of the  $i$ th joint. Since the generated torques of motors are given by [8]

$$T_{ei} = K_{ti} \left[ f_i(\theta_i) \ell_{1i} + f_i\left(\theta_i - \frac{2\pi}{3}\right) \ell_{2i} + f_i\left(\theta_i - \frac{4\pi}{3}\right) \ell_{3i} \right] \quad (5)$$

where  $K_{ti}$  is the torque constant of the  $i$ th motor, the  $i$ th joint torque  $T_i$  is then

$$T_i = N_i K_{ti} u_i, \quad j = 1, \dots, n \quad (6)$$

where  $u_i \triangleq [f_i(\theta_i) \ell_{1i} + f_i(\theta_i - 2\pi/3) \ell_{2i} + f_i(\theta_i - 4\pi/3) \ell_{3i}]$ .

*Remark:* We note that the torque generated by (6) is quite complicated due to the nonlinear coupling of phase currents. We can also use other models to describe three-phase BLDCM's, for example, models obtained from the rotor-fixed reference frame or from  $d$ - $q$  transformation [10]. However, the relations between torque and current are still nonlinear. This fact constitutes the major difference, compared with the brushed counterpart.

After the dynamic equations of each BLDCM are obtained, the dynamics of the robot manipulator are governed by [18]

$$\sum_{j=1}^n D_{ij} \ddot{q}_j + J_i \ddot{q}_i + \sum_{j=1}^n \sum_{k=1}^n D_{ijk} \dot{q}_j \dot{q}_k + G_i = T_i, \quad i = 1, \dots, n \quad (7)$$

where

$q_i, \dot{q}_i, \ddot{q}_i$	position, velocity, and acceleration of joint $i$ ,
$J_i$	reflected actuator inertia of joint $i$ ,
$T_i$	torque (or force) acting at joint $i$ ,
$D_{ii}, D_{ij}$	effective and coupling inertias,

$D_{ijj}, D_{ijk}$  coefficients of centripetal and Coriolis forces,  
 $G_i$  gravity force.

Now we let  $\mathcal{I}_i \triangleq [\ell_{1i}, \ell_{2i}, \ell_{3i}]^T$ ,  $F_i(\theta_i) \triangleq [f_i(\theta_i), f_i(\theta_i - 2\pi/3), f_i(\theta_i - 4\pi/3)]^T$ , and  $V_i \triangleq [v_{1i}, v_{2i}, v_{3i}]^T$ . Then (1) can be written as

$$R_{si} \mathcal{I}_i + L_{si} \dot{\mathcal{I}}_i + K_{ei} F_i(\theta_i) \dot{\theta}_i = V_i \quad i = 1, \dots, n. \quad (8)$$

The compact form of (7) and (8) can be expressed as

$$[D(\mathbf{q}) + J] \ddot{\mathbf{q}} + B(\mathbf{q}, \dot{\mathbf{q}}) \dot{\mathbf{q}} + G(\mathbf{q}) = K_N \mathbf{u} \quad (9)$$

$$R_s \mathbf{I} + L_s \dot{\mathbf{I}} + \mathbf{F}(\theta) K_e \dot{\mathbf{q}} = \mathbf{V} \quad (10)$$

where  $\mathbf{q} = [q_1 \ q_2 \ \dots \ q_n]^T \in R^n$ ;  $\mathbf{u} = [u_1, \dots, u_n]^T \in R^n$ ;  $\mathbf{I} = [\mathcal{I}_1^T, \dots, \mathcal{I}_n^T]^T \in R^{3n}$ ;  $K_N \triangleq \text{diag}[N_i K_{ti}]$ ;  $K_e \triangleq \text{diag}[N_i K_{ei}]$ ;

$$\mathbf{F}(\theta) \triangleq \begin{bmatrix} F_1(\theta_1) & 0 & \dots & 0 & 0 \\ 0 & F_2(\theta_2) & \dots & 0 & 0 \\ \vdots & \vdots & \ddots & \vdots & \vdots \\ 0 & 0 & \dots & 0 & F_n(\theta_n) \end{bmatrix}$$

$D(\mathbf{q})$  is the manipulator mass matrix, which is a symmetric positive definite matrix;  $B(\mathbf{q}, \dot{\mathbf{q}}) \dot{\mathbf{q}}$  represents the centripetal and Coriolis force;  $G(\mathbf{q})$  denotes the gravitational force;  $J$  is the actuator inertia matrix. While  $D(\mathbf{q})$ ,  $B(\mathbf{q}, \dot{\mathbf{q}})$ , and  $G(\mathbf{q})$  are nonlinear functions,  $K_N$ ,  $R_s$ ,  $L_s$ ,  $K_e$ , and  $J$  are positive definite constant diagonal matrices. We note that the matrix  $(\dot{D} - 2B)$  is skew symmetric.

### III. DERIVATION OF THE CONTROL LAW

The considered adaptive controller design problem is as follows: For any given desired bounded trajectories  $\mathbf{q}_d$ ,  $\dot{\mathbf{q}}_d$ , and  $\mathbf{q}_d^{(3)} \in R^n$ , with some or all of the manipulator and BLDCM parameters unknown, derive a controller for the BLDCM stator phase voltages  $\mathbf{V}$  such that the manipulator position vector  $\mathbf{q}(t)$  tracks  $\mathbf{q}_d(t)$ . In the following development, it is assumed that  $\dot{\mathbf{q}}$ ,  $\mathbf{q}$ , and  $\mathbf{I}$  are measurable and the exact values of the robotic functions  $D(\mathbf{q})$ ,  $B(\mathbf{q}, \dot{\mathbf{q}}) \dot{\mathbf{q}}$ , and  $G(\mathbf{q})$  and BLDCM dynamic coefficients matrices  $J$  and  $K_N$ , and constants  $R_s$ ,  $L_s$ ,  $K_e$  are not available.

Considering the dynamic model (9) and (10), we are only free to specify the motor stator phase voltages  $\mathbf{V}$ . Unlike the dynamic model of a robot at the torque input level, the virtual force  $K_N \mathbf{u}$  in (9) cannot be synthesized directly. Instead, it

is the nonlinear output of the BLDCM stator phase currents. In accordance with integrator backstepping technique [12], the design procedure is organized as a two-step process. First, the vector  $\mathbf{u}$  is regarded as a control variable for subsystem (9) and an "embedded" control input  $\mathbf{u}_d$  is designed so that the tracking goal may be achieved. Secondly,  $\mathbf{V}$  are designed such that  $\mathbf{u}$  tracks  $\mathbf{u}_d$ . In turn, this allows  $\mathbf{q}(t)$  to track  $\mathbf{q}_d(t)$ .

In this paper the subsystems of (9) and (10) represent the system for which we will design adaptive and robust algorithm. Therefore, (9) is called the *manipulator subsystem* and (10) the *BLDCM subsystem*.

#### A. Adaptive Control for the Manipulator Subsystem

Considering the electrical subsystem dynamics of (10), we are only free to specify the motor stator phase voltages  $\mathbf{V}$ . In other words, the mechanical subsystem dynamics lack a true current level control input. For this reason, we shall add and subtract an embedded vector  $\mathbf{u}_d$  to the right-hand side of (9), as shown:

$$[D(\mathbf{q}) + J]\ddot{\mathbf{q}} + B(\mathbf{q}, \dot{\mathbf{q}})\dot{\mathbf{q}} + G(\mathbf{q}) = K_N \mathbf{u}_d + K_N \tilde{\mathbf{u}} \quad (11)$$

where  $\tilde{\mathbf{u}} \triangleq \mathbf{u} - \mathbf{u}_d$  represents a *fictitious* perturbation to the rigid-link dynamics. The system (11) can then be viewed as a rigid model system with an input disturbance  $K_N \tilde{\mathbf{u}}$ , and is controlled by  $K_N \mathbf{u}_d$ . The synthesis of  $K_N \mathbf{u}_d$  may follow any available design procedures developed at the torque input level.

However, the direct application of design procedures developed at the torque input level to design  $\mathbf{u}_d$  is impaired by the assumption that the electromechanical conversion matrix  $K_N$  is not exactly available, and thus  $\mathbf{u}_d$  cannot be calculated from  $K_N \mathbf{u}_d$ . Therefore, one needs a modified scheme in order to directly generate the signal  $\mathbf{u}_d$ .

To solve this problem, firstly, based on the parameterization technique as in [15], the nonlinear terms  $D$ ,  $B$ , and  $G$  in (9) can be expressed as

$$[D(\mathbf{q}) + J]\ddot{\mathbf{q}} + B(\mathbf{q}, \dot{\mathbf{q}})\dot{\mathbf{q}} + G(\mathbf{q}) = \Phi(\mathbf{q}, \dot{\mathbf{q}}, \ddot{\mathbf{q}})\alpha \quad (12)$$

where  $\Phi(\mathbf{q}, \dot{\mathbf{q}}, \ddot{\mathbf{q}}) \in R^{n \times m}$  is the regressor matrix independent of the dynamic parameters,  $\alpha$  is a constant vector of manipulator inertia parameters.

Following [6], let  $\Phi$  be written as  $\Phi^T = [\phi_1 \ \phi_2 \ \dots \ \phi_n]$ , where  $\phi_i^T$  is the  $i$ th row of  $\Phi$ , and introduce the augmented regressor matrix  $\Phi_a(\mathbf{q}, \dot{\mathbf{q}}, \ddot{\mathbf{q}})$  defined as

$$\Phi_a(\mathbf{q}, \dot{\mathbf{q}}, \ddot{\mathbf{q}}) \triangleq \begin{bmatrix} \phi_1^T & 0 & \dots & 0 & 0 \\ 0 & \phi_2^T & \dots & 0 & 0 \\ \vdots & \vdots & \ddots & \vdots & \vdots \\ 0 & 0 & \dots & 0 & \phi_n^T \end{bmatrix}$$

then

$$\begin{aligned} K_N^{-1}\Phi\alpha &= K_N^{-1}\Phi_a\alpha_a \\ &= \Phi_a K_{Na}^{-1}\alpha_a \\ &= \Phi_a\alpha_{ak} \end{aligned} \quad (13)$$

where  $K_{Na} \triangleq \text{diag}[k_{Ni}I_m]$ ,  $\alpha_a^T \triangleq [\alpha^T \alpha^T \ \dots \ \alpha^T]$  is a corresponding augmented inertia parameter vector,  $\alpha_{ak}^T \triangleq [k_{N1}^{-1}\alpha^T \ k_{N2}^{-1}\alpha^T \ \dots \ k_{Nn}^{-1}\alpha^T]$ .

We suppose only that the parameter vector  $\alpha_{ak}$  is *uncertain*. Following the results of [21], the desired  $\mathbf{u}_d$  is then synthesized by

$$\mathbf{u}_d = \Phi_a(\mathbf{q}, \dot{\mathbf{q}}_d, \ddot{\mathbf{q}}_d)\hat{\alpha}_{ak} - \gamma^2\Gamma(\mathbf{w} + \kappa\tilde{\mathbf{q}}) \quad (14)$$

where  $\tilde{\mathbf{q}} \triangleq \mathbf{q} - \mathbf{q}_d$  is the joint tracking error;  $\Gamma$  is an arbitrary positive definite constant diagonal matrix;  $\gamma$  and  $\kappa$  are positive constants;  $\mathbf{w}$  is an intermediate vector synthesized by

$$\dot{\mathbf{w}} = -2\gamma\mathbf{w} + \gamma^2\dot{\tilde{\mathbf{q}}}. \quad (15)$$

The adaptive law for adjusting  $\hat{\alpha}_{ak}$  is given by

$$\dot{\hat{\alpha}}_{ak} = \dot{\alpha}_{ak} = -\sigma\Phi_a^T\mathbf{z} \quad (16)$$

$$\mathbf{z} \triangleq \dot{\tilde{\mathbf{q}}} - \frac{1}{\gamma}\mathbf{w} + \frac{\kappa}{\gamma}\tilde{\mathbf{q}} \quad (17)$$

where  $\tilde{\alpha}_{ak} \triangleq \hat{\alpha}_{ak} - \alpha_{ak}$  denotes the parameter error vector.

*Remark:* We will show later that  $\mathbf{u}_d$  given by the control law (14) and (15) and adaptive law (16) and (17) is actually embedded inside of an overall control strategy which is designed at  $\mathbf{V}$ , the motor stator phase voltages.

We now show that this  $\mathbf{u}_d$  could guarantee position tracking for the manipulator subsystem if the term  $\tilde{\mathbf{u}}$  was equal to zero.

Substituting (14) into (11), one obtains the joint position error equation:

$$\begin{aligned} K_N^{-1}[D(\mathbf{q}) + J]\ddot{\tilde{\mathbf{q}}} &= -\gamma^2\Gamma\mathbf{w} - \kappa\gamma^2\Gamma\tilde{\mathbf{q}} + \tilde{\mathbf{u}} - K_N^{-1}B(\mathbf{q}, \dot{\mathbf{q}})\dot{\tilde{\mathbf{q}}} \\ &\quad - K_N^{-1}B_d\dot{\tilde{\mathbf{q}}} + \Phi_a\tilde{\alpha}_{ak} \end{aligned} \quad (18)$$

where  $B_d\dot{\tilde{\mathbf{q}}} \triangleq B(\mathbf{q}, \dot{\mathbf{q}})\dot{\mathbf{q}}_d - B(\mathbf{q}, \dot{\mathbf{q}})\dot{\mathbf{q}}_d$ . It can be shown that  $B_d$  is a uniformly bounded matrix because  $\dot{\mathbf{q}}_d$  is uniformly bounded.

Introducing a state vector  $\mathbf{x}^T \triangleq [\tilde{\mathbf{q}}^T, \mathbf{w}^T, \tilde{\alpha}_{ak}^T]$ , then (18) can be expressed in state space as

$$\dot{\mathbf{x}} = -A\mathbf{x} + C[\tilde{\mathbf{u}} - K_N^{-1}B(\mathbf{q}, \dot{\mathbf{q}})\dot{\tilde{\mathbf{q}}} - K_N^{-1}B_d\dot{\tilde{\mathbf{q}}} + \Phi_a\tilde{\alpha}_{ak}] \quad (19)$$

where (15) is incorporated to obtain

$$A \triangleq \begin{bmatrix} 0 & \gamma^2(D+J)^{-1}K_N\Gamma & \kappa\gamma^2(D+J)^{-1}K_N\Gamma \\ -\gamma^2E & 2\gamma E & 0 \\ -E & 0 & 0 \end{bmatrix}$$

and

$$C \triangleq \begin{bmatrix} (D+J)^{-1}K_N \\ 0 \\ 0 \end{bmatrix}$$

where  $E$  denotes the identity matrix.

An important design procedure is to find a pair of positive definite matrices  $P$  and  $Q$  such that  $\frac{1}{2}(PA + A^T P) = Q$ . A possible choice is given by

$$P \triangleq \begin{bmatrix} (D+J) & -\frac{1}{\gamma}(D+J) & \frac{\kappa}{\gamma}(D+J) \\ -\frac{1}{\gamma}(D+J) & K_N\Gamma & 0 \\ \frac{\kappa}{\gamma}(D+J) & 0 & \kappa\gamma^2K_N\Gamma \end{bmatrix}$$

and

$$Q = \gamma Q_1 \triangleq \gamma \begin{bmatrix} \left(1 - \frac{\kappa^2}{\gamma}\right)(D+J) & -\frac{D+J}{\gamma} & 0 \\ \frac{D+J}{\gamma} & \gamma K_N & 0 \\ 0 & 0 & \kappa^2 K_N \Gamma \end{bmatrix}.$$

Since the eigenvalues of  $D$  are uniformly bounded for all  $\mathbf{q}$ , therefore, by choosing a sufficient large  $\gamma$ , one can make  $P$ ,  $Q_1$ , and therefore  $Q$ , positive definite. Thus we have

$$\lambda_p \|\mathbf{x}\|^2 \leq \mathbf{x}^T P \mathbf{x}$$

and

$$\gamma \lambda_q \|\mathbf{x}\|^2 \leq \mathbf{x}^T Q \mathbf{x}. \quad (20)$$

where  $\lambda_p$  and  $\lambda_q$  denote the smallest eigenvalues of the matrices  $P$  and  $Q_1$ .

Stability of the closed-loop system described by (19) and (16), when  $\tilde{\mathbf{u}}$  is zero, is established by the following lemma.

*Lemma:* In the closed-loop system described by (19) and (16), all signals are bounded and  $\lim_{t \rightarrow \infty} \tilde{\mathbf{q}} = 0$ , provided  $\tilde{\mathbf{u}} = 0$  and  $\gamma$  initially satisfies

$$\gamma \lambda_q > 3 \|B_d\| + 2\vartheta \|\delta_d\| + 2\vartheta \sqrt{\frac{\lambda_2}{\lambda_1}} \|\mathbf{x}_\alpha(0)\|, \quad (21)$$

where  $\lambda_p$  is defined in (20);  $\lambda_1$  and  $\lambda_2$  are defined in (43);  $\mathbf{x}_\alpha^T = [\mathbf{x}^T \tilde{\alpha}_{ak}^T]$ .

*Proof:* See Appendix A.

### B. Adaptive Sliding Mode Control for BLDCM Subsystem

Since  $\tilde{\mathbf{u}}$  in (19) and (16) is not equal to zero in general, as the second step in the procedure, the objective for the BLDCM subsystem is to design stator phase voltage inputs  $\mathbf{V}$ , forcing  $\tilde{\mathbf{u}}$  to zero, such that  $\mathbf{u}_d$ , a synthesized vector, acts as the dominating control signals to the mechanical dynamics of (11).

However,  $u_i$  is defined as  $u_i \triangleq [f_i(\theta_i)\ell_{1i} + f_i(\theta_i - 2\pi/3)\ell_{2i} + f_i(\theta_i - 4\pi/3)\ell_{3i}]$ , which is nonlinearly coupled by stator phase currents. This fact, compared with the brushed motors, constitutes the major difficulty for the controller design. In order to use the backstepping technique, we wish to find the ‘‘embedded’’ stator phase currents  $\ell_{1i}^d, \ell_{2i}^d, \ell_{3i}^d$  so that  $\ell_{ki} \rightarrow \ell_{ki}^d$  ( $k = 1, 2, 3$ ) implies  $u_i \rightarrow u_{di}$ , where  $u_{di} \in \mathbf{u}_d$ . In such a case, the control problem would become direct, i.e., design stator phase voltages  $\mathbf{V}$  such that stator phase currents  $\mathbf{I}$  track the embedded stator currents  $\mathbf{I}^d$ , and therefore  $\mathbf{u} \rightarrow \mathbf{u}_d$ .

In order to do so, using the linearizing technique developed in [8], let the embedded stator phase currents  $\ell_{1i}^d, \ell_{2i}^d, \ell_{3i}^d$  be defined as

$$\ell_{ki}^d \triangleq u_{di} h_{ki}(\theta_i), \quad k = 1, 2, 3, \quad i = 1, \dots, n. \quad (22)$$

where  $h_{ki}$  ( $k = 1, 2, 3$ ) are an arbitrary functions having the following properties:

$$\sum_{k=1}^3 f_i \left( \theta_j - 2\pi \frac{k-1}{3} \right) h_{ki}(\theta_i) = 1 \quad (23)$$

$$\sum_{k=1}^3 h_{ki}(\theta_i) = 0 \quad (24)$$

$$h_{ki}(\theta_i + 2\pi) = h_{ki}(\theta_i). \quad (25)$$

It can easily be verified [8] that the relation  $u_{di} = [f_i(\theta_i)\ell_{1i}^d + f_i(\theta_i - 2\pi/3)\ell_{2i}^d + f_i(\theta_i - 4\pi/3)\ell_{3i}^d]$  holds. Therefore,  $\mathbf{I}^d$  can be obtained by (22). Since  $f_i$ ,  $i = 1, \dots, n$ , are assumed known,  $h_{ki}$  can be explicitly constructed. The details of constructing  $h_{ki}$  was discussed in [8] and briefly listed in Appendix B for completeness.

We are now ready to propose a control law to compensate  $\tilde{\mathbf{u}}$  through the BLDCM subsystem. For synthesizing such a controller, various control approaches may be employed. In this paper, we only focus on sliding mode methods. For the general theory of sliding mode control, the reader is referred to [20]. To employ the sliding mode method, throughout the following development, we suppose that the electrical parameters  $R_s$ ,  $L_s$ , and  $K_e$  are all of uncertain values. However, there exist  $L_s^o$ ,  $R_s^o$ , and  $K_e^o$ , all known, such that

$$\begin{aligned} \|L_s^o - L_s\| &\leq \delta_1 \\ \|R_s^o - R_s\| &\leq \delta_2 \\ \|K_e^o - K_e\| &\leq \delta_3. \end{aligned} \quad (26)$$

Forcing  $\tilde{\mathbf{I}} \triangleq \mathbf{I} - \mathbf{I}_d = 0$ , an sliding surface is chosen as

$$\tilde{\mathbf{I}} = 0. \quad (27)$$

With the above in mind, an adaptive sliding mode control law is then synthesized by

$$\begin{aligned} \mathbf{V} &= L_s^o \dot{\mathbf{I}}_d + R_s^o \mathbf{I}_d + \mathbf{F}(\theta) K_e^o \dot{\mathbf{q}}_d \\ &\quad - (\hat{\delta}_1 \|\dot{\mathbf{I}}_d\| + \hat{\delta}_2 \|\mathbf{I}_d\| + \hat{\delta}_3 \|\mathbf{F}(\theta)\| \|\dot{\mathbf{q}}_d\|) \text{sgn}(\tilde{\mathbf{I}}) \end{aligned} \quad (28)$$

$$\hat{\delta}_1 = \eta_1 \|\tilde{\mathbf{I}}_d\| \|\tilde{\mathbf{I}}\| \quad (29)$$

$$\hat{\delta}_2 = \eta_2 \|\mathbf{I}_d\| \|\tilde{\mathbf{I}}\| \quad (30)$$

$$\hat{\delta}_3 = \eta_3 \|\dot{\mathbf{q}}_d\| \|\mathbf{F}(\theta)\| \|\tilde{\mathbf{I}}\| \quad (31)$$

where  $\mathbf{I}_d = [I_{d1}^T, \dots, I_{dn}^T]^T$ ,  $I_{di} \triangleq [\ell_{1i}^d, \ell_{2i}^d, \ell_{3i}^d]^T$ , and  $\ell_{ki}^d$  ( $k = 1, 2, 3; i = 1, \dots, n$ ) are defined in (22);  $\eta_i$  ( $i = 1, 2, 3$ ) are constants, determining the rates of the adaptations.

*Remark:* Note that the embedded stator phase current  $\mathbf{I}^d$ , calculated by (22) and (14), is embedded inside the voltage  $\mathbf{V}$ . We also note that two different control strategies (i.e., adaptive and adaptive sliding mode) are fused, the controller is, therefore, referred to as a *hybrid* integrator backstepping controller.

The dynamics given by (9), (10), (14), (22), and (28) represent the electromechanical closed-loop system for which the stability is performed. The structure of the controller given by (35) is sketched in Fig. 1. The controller consists of two parts. In the first part,  $\mathbf{u}_d$  represents an *embedded* control input, which may be viewed as an adaptive controller that ensures the convergence of tracking error if the actuator dynamics are not present. In the second part, the input voltage  $\mathbf{V}$  regulates the real phase stator currents about the *embedded* currents and therefore attempts to provide the control voltages necessary to make the desired motions.

The following theorem shows that the proposed sliding mode voltage controller provides good link position tracking for the closed-loop electromechanical system.

*Theorem 1:* If the robust control voltages  $\mathbf{V}$  given by (28) are applied to the electromechanical dynamics of (9) and (10), then all closed-loop signals are bounded and  $\lim_{t \rightarrow \infty} \tilde{\mathbf{q}} = 0$ , provided  $\gamma$  initially satisfies

$$\gamma \lambda_q > 3 \|B_d\| + \mu + 2\vartheta \|\dot{\mathbf{q}}_d\| + 2\vartheta \sqrt{\frac{\lambda_{v2}}{\lambda_{v1}}} \|\mathbf{x}_v(0)\| \quad (32)$$

where  $\lambda_q$  is defined in (20);  $\lambda_{v1}$ ,  $\lambda_{v2}$ , and  $\mathbf{x}_v$ , are defined in (52) while

$$\mu \triangleq \frac{\beta^2}{4\lambda_r}$$

$$\beta = (3\alpha_f + \alpha_k)$$

and

$$\lambda_r \triangleq \inf \frac{\tilde{\mathbf{I}}^T R_s \tilde{\mathbf{I}}}{\|\tilde{\mathbf{I}}\|^2}$$

*Proof:* See Appendix C.

*Remarks:*

- 1) It should be noted that the control law given by (28)–(31) depends on the calculation of  $\tilde{\mathbf{I}}_d$  and therefore  $\dot{\mathbf{u}}_d$ . Since  $\mathbf{u}_d$  in (14) only involves the position feedback  $\mathbf{q}$ , the derivative of  $\mathbf{u}_d$  therefore, only needs velocity feedback  $\dot{\mathbf{q}}$ . This is the motivation of synthesizing  $\mathbf{u}_d$  in (14). Actually, the development of  $\mathbf{u}_d$  is based on the *lead-plus-bias* controller proposed in [22] such that the velocity feedback is avoided. In this case, the adaptive control law (28)–(31) for the cascade control system merely requires the measurements of  $\mathbf{I}$ ,  $\mathbf{q}$ , and  $\dot{\mathbf{q}}$ .
- 2) Unlike conventional sliding mode control schemes, we note that in the control law (28)–(31), upper bounds on  $\delta_1$ ,  $\delta_2$ , and  $\delta_3$  are not assumed to be available and suitable integral updated laws are introduced so that  $\hat{\delta}_1$ ,  $\hat{\delta}_2$ , and  $\hat{\delta}_3$  grow until they reach to whatever levels are necessary to cancel the nonlinear dynamics.
- 3) If  $I_j$  is a scalar and  $F_j = 1$  in (8), then the BLDCM dynamic equation (10) is the same as that of its brushed counterpart [18]. Hence, the developed algorithm is also applicable to the robots driven by brush dc motors. Therefore, a united formula has been proposed for both brushed and BLDCM's.
- 4) The control law (28) involves the discontinuous functions and may result in chatter. However, in this case, the chattering signal is the voltage. Due to the direct current nature of the driver and the physical winding constraint, a sliding mode control approach seems appropriate for synthesize voltage. Indeed there exist several theoretical and experimental results that support the idea of sliding mode control for BLDCM's [9]. If the chattering effects were to be eliminated, it would be possible (as suggested by [15]), by smoothing out the control discontinuity in a thin boundary layer neighboring the sliding surface  $E(t) = \{\mathbf{I}, \|\tilde{\mathbf{I}}\| \leq \varepsilon\}$ , where  $\varepsilon > 0$  is the boundary layer thickness. This is achieved by replacing  $\text{sgn}(\tilde{\mathbf{I}})$  in (28) as

$$\pi(\tilde{\mathbf{I}}) = \begin{cases} \text{sgn}(\tilde{\mathbf{I}}), & \text{if } \|\tilde{\mathbf{I}}\| > \varepsilon \\ \frac{\tilde{\mathbf{I}}}{\varepsilon} & \text{if } \|\tilde{\mathbf{I}}\| \leq \varepsilon. \end{cases}$$

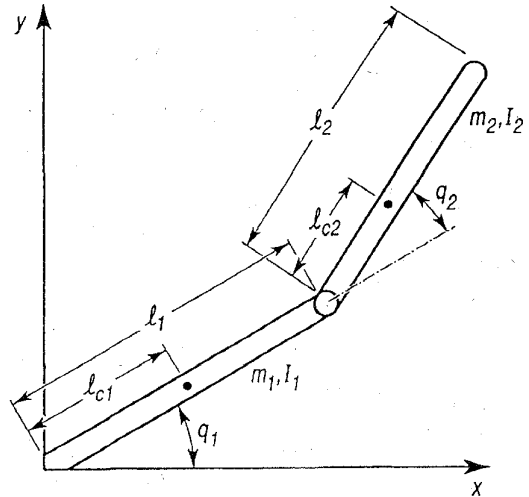


Fig. 2. Two-link manipulator.

It is clear that a continuous control law is defined for any  $\varepsilon$ . In this case, however, the way the performance changes for the closed-loop electromechanical system is worthy of further investigations.

#### IV. A SIMPLIFIED ALGORITHM

From (28) we need to calculate  $\tilde{\mathbf{I}}_d$ , and therefore,  $\dot{\mathbf{u}}_d$ , i.e.,

$$\dot{\mathbf{u}}_d = \frac{d}{dt} [\Phi_a(\mathbf{q}, \dot{\mathbf{q}}_d, \ddot{\mathbf{q}}_d) \hat{\alpha}_{ak}] - \gamma^2 \Gamma (\dot{\mathbf{w}} + \kappa \dot{\mathbf{q}})$$

where  $(d/dt)(\Phi_a \hat{\alpha}_{ak}) = \dot{\Phi}_a \hat{\alpha}_{ak} + \Phi_a \dot{\hat{\alpha}}_{ak}$ . The computation of  $\dot{\Phi}_a$  may be challenging. It seems that there are no reports on how to *recursively* compute it for a general  $n$ -link manipulator in the literature. If such an algorithm were developed, it might be computationally expensive to update  $\dot{\Phi}_a$ . To avoid the intensive computation of  $\dot{\Phi}_a$ , we simply substitute

$$\dot{\mathbf{u}}_m \triangleq -\gamma^2 \Gamma (\dot{\mathbf{w}} + \kappa \dot{\mathbf{q}}) \quad (33)$$

for  $\dot{\mathbf{u}}_d$  since the feedback signal  $\mathbf{u}_m = -\gamma^2 \Gamma (\dot{\mathbf{w}} + \kappa \dot{\mathbf{q}})$  plays a vital role in the stability of the closed-loop system whereas the effect of the feedforward signal  $\mathbf{u}_f \triangleq \Phi_a(\mathbf{q}, \dot{\mathbf{q}}_d, \ddot{\mathbf{q}}_d) \hat{\alpha}_{ak}$  is relatively minor. Equation (33) implies that the BLDCM subsystem becomes a low-pass filter with respect to the feedforward signal  $\mathbf{u}_f$ . The feedback signal  $\mathbf{u}_m$  still passes the actuator subsystem without distortion. In this case, the embedded stator phase currents are modified as

$$\ell_{ki}^m \triangleq u_{mi} h_{ki}(\theta_i), \quad k = 1, 2, 3, \quad i = 1, \dots, n. \quad (34)$$

The adaptive sliding mode control law (28)–(31) is correspondingly modified as

$$\mathbf{V} = L_s^o \dot{\mathbf{I}}_m + R_s^o \mathbf{I}_d + \mathbf{F}(\theta) K_e^o \dot{\mathbf{q}}_d - [\hat{\delta}_1 \|\dot{\mathbf{I}}_m\| + \hat{\delta}_2 \|\mathbf{I}_d\| + \hat{\delta}_3 \|\mathbf{F}(\theta)\| \|\dot{\mathbf{q}}_d\|] \text{sgn}(\tilde{\mathbf{I}}) \quad (35)$$

$$\dot{\hat{\delta}}_1 = \eta_1 \|\dot{\mathbf{I}}_m\| \|\tilde{\mathbf{I}}\| \quad (36)$$

$$\dot{\hat{\delta}}_2 = \eta_2 \|\mathbf{I}_d\| \|\tilde{\mathbf{I}}\| \quad (37)$$

$$\dot{\hat{\delta}}_3 = \eta_3 \|\dot{\mathbf{q}}_d\| \|\mathbf{F}(\theta)\| \|\tilde{\mathbf{I}}\|. \quad (38)$$

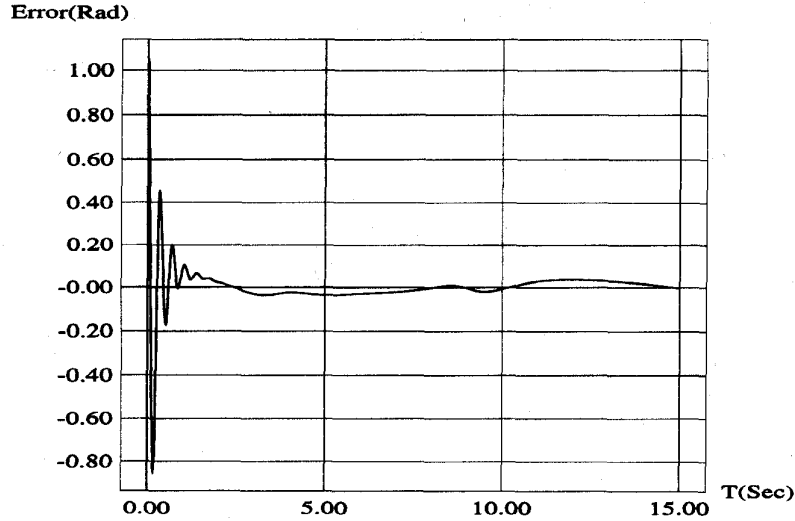


Fig. 3. Tracking error of joint one using the algorithm (28)–(31).

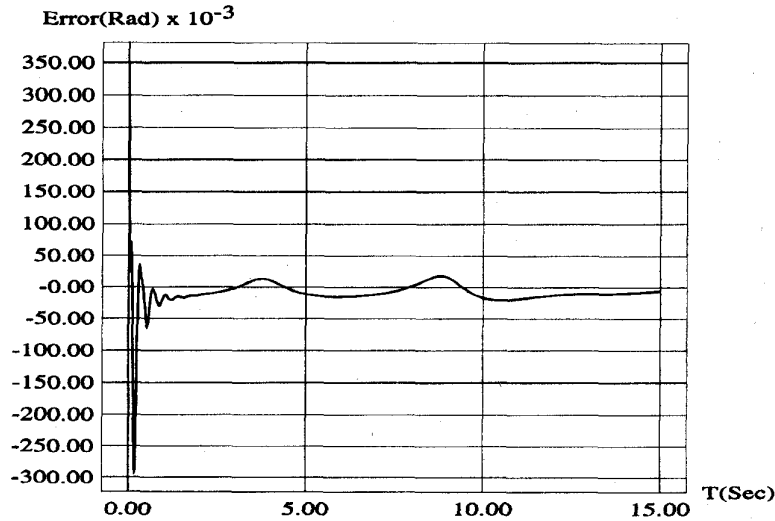


Fig. 4. Tracking error of joint two using the algorithm (28)–(31).

The stability of the closed-loop electromechanical system is therefore stated in the following theorem.

*Theorem 2:* In the closed-loop electromechanical dynamics described by (9), (10), and (35), if the estimated inertia parameters  $\hat{\alpha}_{ak}$  are bounded, then all closed-loop signals are bounded and  $\lim_{t \rightarrow \infty} \tilde{q} = 0$ , provided  $\gamma$  initially satisfies

$$\gamma \lambda_q > 3 \|B_d\| + \mu_1 + 2\vartheta \|\dot{q}_d\| + 2\vartheta \sqrt{\frac{\lambda_{v2}}{\lambda_{v1}}} \|x_m(0)\| \quad (39)$$

where  $\lambda_q$  is defined in (20);  $\lambda_{v1}$  and  $\lambda_{v2}$  are defined in (52), and  $x_m$  is defined in (61) while

$$\begin{aligned} \mu_1 &\triangleq \frac{\beta_1^2}{4\lambda_r} \\ \beta_1 &= (3\alpha_f + \zeta_1 + \alpha_k) \end{aligned}$$

and

$$\lambda_r \triangleq \inf \frac{\tilde{\mathbf{I}}^T R_s \tilde{\mathbf{I}}}{\|\tilde{\mathbf{I}}\|^2}.$$

*Proof:* See Appendix D.

*Remark:* The validity of the simplified algorithm depends on the boundedness of the estimated inertia parameters  $\hat{\alpha}_{ak}$ . Although the boundedness of  $\hat{\alpha}_{ak}$  is verified in simulation results, the strict proof in theory remains an open question. However, as long as  $\hat{\alpha}_{ak}$  is uniformly bounded, the stability of the closed-loop, using  $\hat{u}_m$  instead of  $u_d$ , can be guaranteed, and the simplified algorithm is of the same complexity as the algorithm by Slotine and Li [15].

## V. A SIMULATION EXAMPLE

As an illustration, we will apply both the algorithm (28)–(31) and the simplified algorithm (35)–(38) to a two-link robot arm driven directly by the BLDCM shown in Fig. 2. We should note that although a robot manipulator must have a three degree-of-freedom, at least in order to move to an arbitrary point in space, a two degree-of-freedom system,

however, is sufficient to examine the validity of the control strategy.

The robot model is described by (9) and (10). A parameterization scheme for this robot is given in [6]

$$\begin{aligned}\alpha_1 &= m_2 l_1^2 + m_l l_1^2 + I_1 + I_2 + J_1 + I_l \\ \alpha_2 &= I_2 + J_2 + I_l \\ \alpha_3 &= I_2 + I_l \\ \alpha_4 &= m_2 l_1 (l_{c2} + l_2) + m_l l_1 (l_{cl} + l_2) \\ \alpha_5 &= m_2 l_1 + m_1 (l_1 + l_{c1}) + m_l l_1 \\ \alpha_6 &= m_2 (l_2 + l_{c2}) + m_l (l_2 + l_{cl})\end{aligned}\quad (40)$$

where  $m_l$  is the mass of the end-effector and load,  $I_l$  is the inertia of the end-effector and load,  $l_{cl}$  is the mass  $m_l$  center of gravity coordinate,  $J_1$ ,  $J_2$  are the rotor inertias.

With this parameterization,  $\Phi(\mathbf{q}, \dot{\mathbf{q}}_d, \ddot{\mathbf{q}}_d)$  in (12) has components

$$\begin{aligned}\phi_{11} &= \ddot{q}_{d1} \\ \phi_{12} &= 0 \\ \phi_{13} &= \ddot{q}_{d2} \\ \phi_{14} &= \cos(q_2)(2\ddot{q}_{d1} + \ddot{q}_{d2}) \\ &\quad - \sin(q_2)(\dot{q}_{d2}^2 + 2\dot{q}_{d1}\dot{q}_{d2}) \\ \phi_{15} &= g \cos(q_1) \\ \phi_{16} &= g \cos(q_1 + q_2) \\ \phi_{21} &= 0 \\ \phi_{22} &= \ddot{q}_{d2} \\ \phi_{23} &= \ddot{q}_{d1} \\ \phi_{24} &= \cos(q_2)\ddot{q}_{d1} + \sin(q_2)\dot{q}_{d1}^2 \\ \phi_{25} &= 0 \\ \phi_{26} &= g \cos(q_1 + q_2).\end{aligned}\quad (41)$$

The values of the manipulator parameters are given by [6]  $l_1 = 0.45$  m,  $m_1 = 100$  kg,  $l_{c1} = 0.15$  m,  $I_1 = 6.25$  kg·m<sup>2</sup>,  $l_2 = 0.20$  m,  $m_2 = 25$  kg,  $l_{c2} = 0.10$  m,  $I_2 = 0.61$  kg·m<sup>2</sup>,  $m_l = 40$  kg,  $l_{cl} = 0.20$  m,  $I_l = 7.68$  kg·m<sup>2</sup>, and the values of BLDCM parameters are:  $f_1(\theta_1) = \sin(\theta_1)$ ,  $f_2(\theta_2) = \sin(\theta_2)$ ,  $L_{s1} = 6.1$  mH,  $R_{s1} = 1.5$  Ω,  $K_{e1} = 0.215$  Nm·A,  $K_{t1} = 0.215$  N·m/A,  $L_{s2} = 6.1$  mH,  $R_{s2} = 1.5$  Ω,  $K_{e2} = 0.215$  N·m/A,  $K_{t2} = 0.215$  N·m/A,  $J_{R1} = 1.9 \times 10^{-4}$  kgm<sup>2</sup>,  $J_{R2} = 1.9 \times 10^{-4}$  kgm<sup>2</sup>. Since the gear ratios are chosen as  $N_1 = N_2 = 100$ , therefore,  $J_1 = 1.9$  kg·m<sup>2</sup>,  $J_2 = 1.9$  kg·m<sup>2</sup>.

We also need to choose the nominal system parameters. Let the uncertainty of the inertia parameters be originated by the varying load  $m_l$ . The electrical parameters are assumed to have 50% uncertainty. The nominal system parameters are given by  $L_{s1} = L_{s2} = 4$  mH,  $R_1 = R_2 = 1.0$  Ω,  $K_{e1} = K_{e2} = 0.1$  N·m/A,  $m_l = 20$  kg.

In this simulation, the desired joint trajectories are chosen to be

$$q_{1d} = q_{2d} = -90^\circ + 52.5(1 - \cos 1.26t).$$

and the initial displacements and velocities are chosen as  $q_1(0) = -30^\circ$ ,  $q_2(0) = -70^\circ$ ,  $\dot{q}_1(0) = \dot{q}_2(0) = 0$ .

*Case 1: Simulation using the controller (28)–(31).*

The embedded  $\mathbf{I}_d$  is synthesized by (14) where  $\kappa = 7$ ,  $\gamma^2 = 19$ ,  $\Gamma = 4I$ , and  $\sigma = 0.8$ . The initial values of  $\hat{\alpha}_{ak}$  are chosen as  $\hat{\alpha}_{ak}(0) = [1.0, 0.35, 0.18, 0.1, 2, 2.3, 1.3, 0.4, 0.2, 0.1, 2.5, 2.6]^T$ . The controller is then synthesized by (28) where  $\eta_1 = 1 \times 10^{-10}$ ,  $\eta_2 = 1 \times 10^{-7}$ , and  $\eta_3 = 1 \times 10^{-7}$ . The initial values of  $\hat{\delta}_i$  are chosen as  $\hat{\delta}_1(0) = 10 \times 10^{-3}$ ,  $\hat{\delta}_2(0) = 10$ , and  $\hat{\delta}_3(0) = 10$ . The results of the simulation are shown in Figs. 3 and 4. Fig. 3 shows the trajectory tracking error of joint one. Fig. 4 shows the trajectory tracking error of joint two. The results of this simulation indicate the expected tracking performance. It should be noted that in the simulation, the tracking performance depends crucially on the choices of  $\kappa$ ,  $\gamma^2$ ,  $\Gamma$ ,  $\sigma$ , and  $\eta_i$ ,  $i = 1, 2, 3$ . The way to find the optimal values needs further investigation.

*Case 2: Simulation using the simplified controller (35)–(38).*

In this case, all the controller parameters in (35)–(38) are chosen as the same as Case 1. The results of the simulation are shown in Figs. 5 and 6. Fig. 5 shows the trajectory tracking error of joint one. Fig. 6 shows the trajectory tracking error of joint two. From these results, we see that the tracking errors have very similar transient patterns as the control (28) is applied. These results coincide with the analysis in Section IV. It should be mentioned that in the simulation the estimated inertia parameters are converged to bounded values.

*Case 3: Simulation using the simplified controller (35)–(38) with unknown disturbances.*

In this case, we assume that the manipulator is subjected to unknown friction and torque disturbances described by

$$T_d = \begin{bmatrix} 0.5 \sin(30t) + 4\dot{q}_1 + 1.5 \operatorname{sgn}(\dot{q}_1) \\ 0.5 \sin(30t) + 4\dot{q}_2 + 1.5 \operatorname{sgn}(\dot{q}_2) \end{bmatrix}$$

and the load  $m_l$  changes as  $m_l = 40 + \Delta m_l$ , where  $\Delta m_l = 5 \cos 0.2t$ . Changes in the load were not accounted for in the controller in order to test the robustness of the controller, i.e., all the parameters in the controller (35)–(38) are still chosen as the same as Case 1. The results of the simulation are shown in Figs. 7 and 8. Fig. 7 shows the trajectory tracking error of joint one. Fig. 8 shows the trajectory tracking error of joint two. We see that the tracking errors still have very similar transient patterns as those results without the external disturbances  $T_d$  and the time-varying load  $m_l$ . These results verify the robustness of the proposed algorithm.

## VI. CONCLUSION

The significance of the work lies in the unique fusion of some existing and some new control techniques to generate a particular controller, suitable for robots actuated with BLDCM's. The control law requires the measurement of only joint positions, velocities and motor stator phase currents. Semi-global stability of the closed-loop system is established in the Lyapunov sense in spite of uncertain mechanical and electrical parameters. Simulations were performed with a two-link example, and simulation results verify the correctness of the proposed scheme.

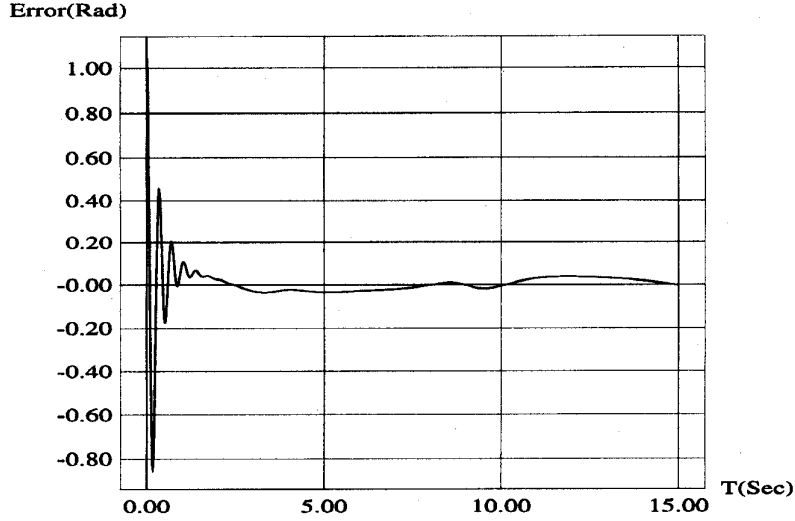


Fig. 5. Tracking error of joint one using the algorithm (35)–(38).

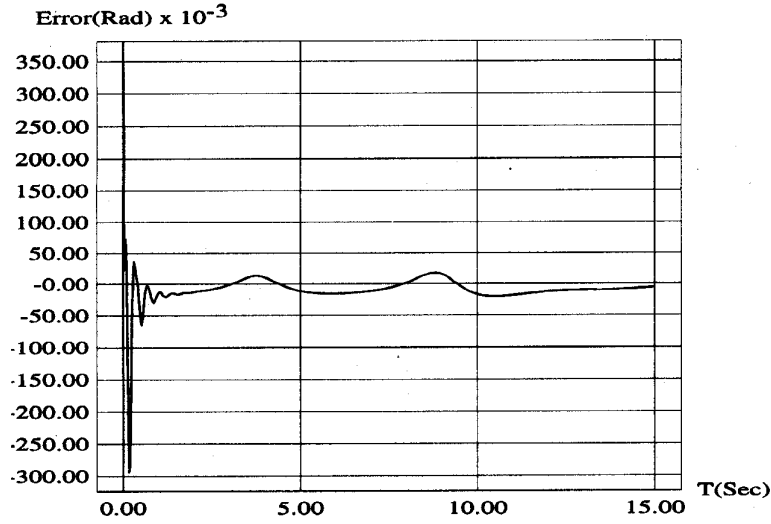


Fig. 6. Tracking error of joint two using the algorithm (35)–(38).

APPENDIX A  
PROOF OF LEMMA 1

Consider a Lyapunov function candidate

$$L_a = \frac{1}{2} [\mathbf{x}^T \tilde{\alpha}_{ak}^T] \begin{bmatrix} P & 0 \\ 0 & \frac{1}{\sigma} E \end{bmatrix} \begin{bmatrix} \mathbf{x} \\ \tilde{\alpha}_{ak} \end{bmatrix} \quad (42)$$

where  $E$  denotes the identity matrix. Given (42), one has

$$\lambda_1 \|\mathbf{x}_\alpha\|^2 \leq L_a \leq \lambda_2 \|\mathbf{x}_\alpha\|^2 \quad (43)$$

where  $\mathbf{x}_\alpha^T \triangleq [\mathbf{x}^T \tilde{\alpha}_{ak}^T]$ ;  $\lambda_1 \triangleq \frac{1}{2} \min \{\lambda_{\min}(P), 1/\sigma\}$ , and  $\lambda_2 \triangleq \frac{1}{2} \max \{\lambda_{\max}(P), 1/\sigma\}$ .

Its time derivative is evaluated along the trajectory of (19) as

$$\begin{aligned} \dot{L}_a = & -\mathbf{x}^T Q \mathbf{x} + \mathbf{x}^T P C [-K_N^{-1} B(\mathbf{q}, \dot{\mathbf{q}}) \dot{\mathbf{q}} \\ & - K_N^{-1} B_d \dot{\mathbf{q}} + \Phi_a \tilde{\alpha}_{ak}] + \frac{1}{2} \mathbf{x}^T \dot{P} \mathbf{x} + \frac{1}{\sigma} \dot{\tilde{\alpha}}_{ak}^T \tilde{\alpha}_{ak}. \end{aligned} \quad (44)$$

When  $\gamma \geq \max \{1, \kappa\}$ , one can write

$$\begin{aligned} -\mathbf{x}^T P C K_N^{-1} B_d \dot{\mathbf{q}} = & - \left( \dot{\mathbf{q}} - \frac{1}{\gamma} \mathbf{w} + \frac{\kappa}{\gamma} \tilde{\mathbf{q}} \right)^T B_d \dot{\mathbf{q}} \\ \leq & 3 \|B_d\| \|\mathbf{x}\|^2 \end{aligned} \quad (45)$$

and

$$\begin{aligned} \frac{1}{2} \mathbf{x}^T \dot{P} \mathbf{x} - \mathbf{x}^T P C K_N^{-1} B(\mathbf{q}, \dot{\mathbf{q}}) \dot{\mathbf{q}} \\ = & \frac{1}{\gamma} (\kappa \tilde{\mathbf{q}} - \mathbf{w})^T [\dot{D} - B(\mathbf{q}, \dot{\mathbf{q}})] \dot{\mathbf{q}} \\ \leq & 2\vartheta \|\dot{\mathbf{q}}\| \|\mathbf{x}\|^2 \end{aligned} \quad (46)$$

where  $\vartheta \|\mathbf{q}\| = \|\dot{D} - B\|$  and identity  $\dot{\mathbf{q}}^T [\frac{1}{2} \dot{D} - B(\mathbf{q}, \dot{\mathbf{q}})] \dot{\mathbf{q}} = 0$  has been used to derive (46). Substituting (20), (45), and (46)



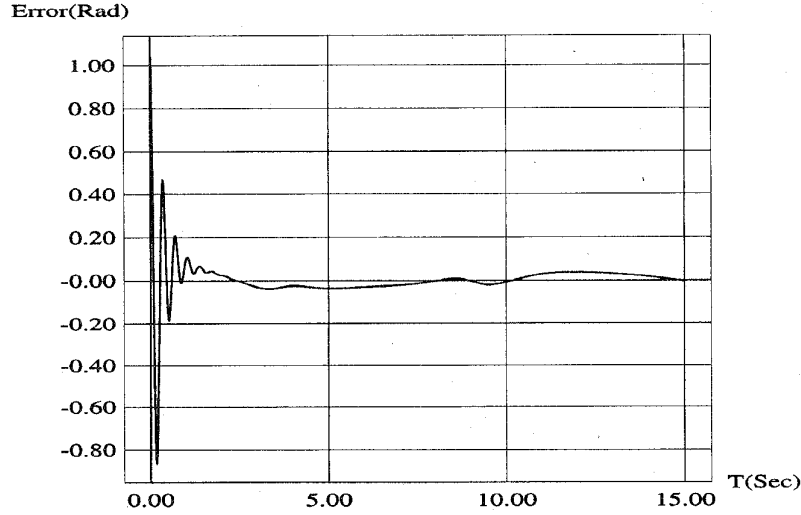


Fig. 7. Tracking error of joint one using the algorithm (35)–(38) with disturbances.

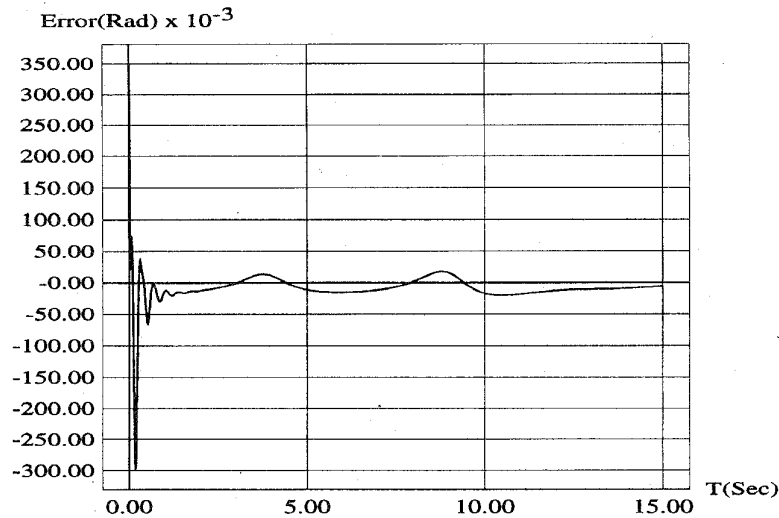


Fig. 8. Tracking error of joint two using the algorithm (35)–(38) with disturbances.

into (44), one obtains

$$\begin{aligned} \dot{L}_a &\leq -(\gamma\lambda_q - 3\|B_d\| - 2\vartheta\|\dot{\mathbf{q}}\|)\|\mathbf{x}\|^2 \\ &\quad + \left( \mathbf{z}^T \Phi_a + \frac{1}{\sigma} \dot{\alpha}_{ak}^T \right) \tilde{\alpha}_{ak} \\ &= -(\gamma\lambda_q - 3\|B_d\| - 2\vartheta\|\dot{\mathbf{q}}\|)\|\mathbf{x}\|^2 \end{aligned} \quad (47)$$

where identity  $\mathbf{x}^T P C \Phi_a \tilde{\alpha}_{ak} = \mathbf{z}^T \Phi_a \tilde{\alpha}_{ak}$  and (16) have been used.

From the definitions of  $\mathbf{x}$  and  $\mathbf{x}_\alpha$ , it is easy to show from (43) that

$$\|\dot{\mathbf{q}}\| \leq \|\mathbf{x}\| + \|\dot{\mathbf{q}}_d\| \leq \|\mathbf{x}_\alpha\| + \|\dot{\mathbf{q}}_d\| \leq \sqrt{\frac{L_a}{\lambda_1}} + \|\dot{\mathbf{q}}_d\| \quad (48)$$

which can be used to place an upper bound for  $\dot{L}_a$  as follows

$$\dot{L}_a \leq -\left( \gamma\lambda_q - 3\|B_d\| - 2\vartheta + \|\dot{\mathbf{q}}_d\| - 2\vartheta\sqrt{\frac{L_a}{\lambda_1}} \right) \|\mathbf{x}\|^2$$

$$\leq -\rho\|\mathbf{x}\|^2 \quad \text{for } L_a < \lambda_1 \left( \frac{\gamma\lambda_q - 2\vartheta + \|\dot{\mathbf{q}}_d\| - 3\|B_d\|}{2\vartheta} \right)^2 \quad (49)$$

where  $\rho$  is a positive constant. When  $L_a < \lambda_1 [(\gamma\lambda_q - 2\vartheta + \|\dot{\mathbf{q}}_d\| - 3\|B_d\|)/2\vartheta]^2$ ,  $L_a$  is positive definite and  $\dot{L}_a$  is negative semi-definite, we have  $L_a(0) \geq L_a$  for all  $t \geq 0$ . From (43), we have  $L_a(0) \leq \lambda_2 \|\mathbf{x}_\alpha(0)\|^2$  which allows (49) to be written as

$$\begin{aligned} \dot{L}_a &\leq -\rho\|\mathbf{x}\|^2 \quad \text{for } \lambda_2 \|\mathbf{x}_\alpha(0)\|^2 \\ &< \lambda_1 \left( \frac{\gamma\lambda_q - 2\vartheta + \|\dot{\mathbf{q}}_d\| - 3\|B_d\|}{2\vartheta} \right)^2 \end{aligned} \quad (50)$$

which yields the gain condition of (21).

To complete the proof, it is necessary to show that  $\hat{\mathbf{q}} \rightarrow 0$  as  $t \rightarrow \infty$ . Since  $\dot{L}_a$  is negative semi-definite,  $\mathbf{x}$  and  $\tilde{\alpha}_{ak}$  are all bounded, which implies that all signals on the right side of (19) are bounded. The boundedness of  $\dot{\mathbf{x}}$  implies that  $\mathbf{x}$  is uniformly continuous. Also, from (50), we can show that

$\mathbf{x} \in \mathcal{L}_2^{3n}$ . Therefore, as a direct consequence of Barbalat's lemma, we have  $\lim_{t \rightarrow \infty} \mathbf{x} = 0$ , which implies the result given in Lemma 1.  $\square$

### APPENDIX B

#### CONSTRUCTION OF $h_{ki}$ [8]

Define the functions  $A_i: R \rightarrow R$  and  $M_i: R \rightarrow R$  by

$$\begin{aligned} A_i(\theta_i) &\triangleq f_i(\theta_i) - f_i\left(\theta_i - \frac{4\pi}{3}\right) \\ M_i(\theta_i) &\triangleq \left| A_i(\theta_i) + \frac{1}{2}A_i\left(\theta_i - \frac{4\pi}{3}\right) \right|^2 \\ &\quad + \frac{3}{4} \left| A_i\left(\theta_i - \frac{4\pi}{3}\right) \right|^2 \end{aligned}$$

Now  $h_i: R \rightarrow R^3$  is defined as

$$h_{ki}(\theta_i) \triangleq \frac{O_{ki}(\theta_i)}{M_i(\theta_i)}, \quad k = 1, 2, 3$$

here, the functions  $O_{ki}(\theta_j): R \rightarrow R$ ,  $k = 1, 2, 3$  are given by

$$\begin{aligned} O_{ki}(\theta_i) &\triangleq A_i \left[ \theta_i - \frac{2\pi(k-1)}{3} \right] \\ &\quad + e_i(\theta_i) A_i \left[ \theta_i - \frac{2\pi(k+1)}{3} \right], \quad k = 1, 2, 3 \end{aligned}$$

where  $e_i: R \rightarrow R$  is an arbitrary periodic function such that

$$e_i(\theta_i + 2\pi) = e_i(\theta_i).$$

Note that the periodic function  $e_i$  can be chosen freely.

### APPENDIX C

#### PROOF OF THEOREM 1

The closed-loop stability is related to a Lyapunov function candidate

$$L(t) = L_a(t) + L_m(t) \quad (51)$$

where  $L_a(t)$  is defined in (42) and

$$L_m(t) \triangleq \frac{1}{2} \tilde{\mathbf{I}}^T L_s \tilde{\mathbf{I}} + \frac{\frac{1}{2} \sum_{i=1}^3 (\delta_i - \hat{\delta}_i)^2}{\eta_i}$$

where  $\delta_i$  is defined in (26) and  $\hat{\delta}_i$  is its estimate. Given (51), one has

$$\lambda_{v1} \|\mathbf{x}_v\|^2 \leq V \leq \lambda_{v2} \|\mathbf{x}_v\|^2 \quad (52)$$

where  $\mathbf{x}_v^T \triangleq [\mathbf{x}^T \tilde{\alpha}_{ak}^T \tilde{\mathbf{I}}^T (\delta_1 - \hat{\delta}_1), (\delta_2 - \hat{\delta}_2), (\delta_3 - \hat{\delta}_3)]$ ;  $\lambda_{v1} \triangleq \frac{1}{2} \min \{ \lambda_{\min}(P), 1/\sigma, \lambda_{\min}(L_s), 1/\eta_i \ (i = 1, 2, 3) \}$  and  $\lambda_{v2} \triangleq \frac{1}{2} \max \{ \lambda_{\max}(P), 1/\sigma, \lambda_{\max}(L_s), 1/\eta_i \ (i = 1, 2, 3) \}$ .

The time derivative of  $L_a(t)$  should not be bounded from above by (47) since  $\tilde{\mathbf{u}}$  is not necessarily an all-zero vector. Instead, an additional term  $\mathbf{x}^T PC \tilde{\mathbf{u}}$  must be added to the right

side of (47) to establish an upper bound for  $\dot{L}_a$  when  $\tilde{\mathbf{u}} \neq 0$ . As a result, one has to write

$$\dot{L}_a \leq -(\gamma\lambda_q - 3\|B_d\| - 2\vartheta\|\dot{\mathbf{q}}\|)\|\mathbf{x}\|^2 + \mathbf{x}^T PC \tilde{\mathbf{u}}. \quad (53)$$

When  $\gamma \geq \max\{1, \kappa\}$ , one can write

$$\mathbf{x}^T PC \tilde{\mathbf{u}} = \left( \dot{\mathbf{q}} - \frac{1}{\gamma} \mathbf{w} + \frac{\kappa}{\gamma} \tilde{\mathbf{q}} \right)^T \mathbf{F}^T(\theta) \tilde{\mathbf{I}} \leq 3\alpha_f \|\mathbf{x}\| \|\tilde{\mathbf{I}}\|. \quad (54)$$

where  $\alpha_f \triangleq \|\mathbf{F}(\theta)\|$ . Consequently,

$$\dot{L}_a \leq -(\gamma\lambda_q - 3\|B_d\| - 2\vartheta\|\dot{\mathbf{q}}\|)\|\mathbf{x}\|^2 + 3\alpha_f \|\mathbf{x}\| \|\tilde{\mathbf{I}}\|. \quad (55)$$

The time derivative of  $L_m(t)$  is evaluated along the trajectory (10) as

$$\begin{aligned} \dot{L}_m &= -\tilde{\mathbf{I}}^T [L_s \dot{\tilde{\mathbf{I}}} + R_s \tilde{\mathbf{I}} + \mathbf{F}(\theta) K_e \dot{\mathbf{q}} - \mathbf{u} + R_s \mathbf{I}_d \mathbf{F}(\theta) K_e \dot{\mathbf{q}}] \\ &\quad + \frac{\sum_{i=1}^3 (\delta_i - \hat{\delta}_i)(-\dot{\hat{\delta}}_i)}{\eta_i}. \end{aligned} \quad (56)$$

Substituting  $\mathbf{V}$  in (56) by the control law (28), one obtains

$$\begin{aligned} \dot{L}_m &\leq -\tilde{\mathbf{I}}^T R_s \tilde{\mathbf{I}} - \tilde{\mathbf{I}}^T \mathbf{F}(\theta) K_e \dot{\mathbf{q}} \\ &\quad + [\delta_1 \|\dot{\tilde{\mathbf{I}}}\| \|\tilde{\mathbf{I}}\| + \delta_2 \|\mathbf{I}_d\| \|\tilde{\mathbf{I}}\| + \delta_3 \|\mathbf{F}(\theta)\| \|\dot{\mathbf{q}}_d\| \|\tilde{\mathbf{I}}\|] \\ &\quad - [\hat{\delta}_1 \|\dot{\tilde{\mathbf{I}}}\| \|\tilde{\mathbf{I}}\| + \hat{\delta}_2 \|\mathbf{I}_d\| \|\tilde{\mathbf{I}}\| + \hat{\delta}_3 \|\mathbf{F}(\theta)\| \|\dot{\mathbf{q}}_d\| \|\tilde{\mathbf{I}}\|] \\ &\quad + \frac{\sum_{i=1}^3 (\delta_i - \hat{\delta}_i)(-\dot{\hat{\delta}}_i)}{\eta_i} \\ &= -\tilde{\mathbf{I}}^T R_s \tilde{\mathbf{I}} - \tilde{\mathbf{I}}^T \mathbf{F}(\theta) K_e \dot{\mathbf{q}} \\ &\leq -\tilde{\mathbf{I}}^T R_s \tilde{\mathbf{I}} + \alpha_k \|\mathbf{x}\| \|\tilde{\mathbf{I}}\| \end{aligned} \quad (57)$$

where  $\alpha_k \triangleq \|K_e\| \|\mathbf{F}\|$ .

Based on (55) and (57),  $\dot{L}$  can be expressed as

$$\begin{aligned} \dot{L} &\leq -(\gamma\lambda_q - 3\|B_d\| - 2\vartheta\|\dot{\mathbf{q}}\|)\|\mathbf{x}\|^2 \\ &\quad + \beta \|\mathbf{x}\| \|\tilde{\mathbf{I}}\| - \tilde{\mathbf{I}}^T R_s \tilde{\mathbf{I}} \\ &\leq -(\gamma\lambda_q - 3\|B_d\| - 2\vartheta\|\dot{\mathbf{q}}\| - \mu)\|\mathbf{x}\|^2 \\ &\quad - \lambda_r (\|\tilde{\mathbf{I}}\| - \nu \|\mathbf{x}\|)^2 \\ &\leq -(\gamma\lambda_q - 3\|B_d\| - 2\vartheta\|\dot{\mathbf{q}}\| - \mu)\|\mathbf{x}\|^2 \end{aligned} \quad (58)$$

where

$$\begin{aligned} \beta &\triangleq (3\alpha_f + \alpha_k) \\ \mu &\triangleq \frac{\beta^2}{4\lambda_r} \\ \nu &\triangleq \frac{\beta}{2\lambda_r} \end{aligned}$$

and

$$\lambda_r \triangleq \inf \frac{\tilde{\mathbf{I}}^T R_s \tilde{\mathbf{I}}}{\|\tilde{\mathbf{I}}\|^2}$$

Similar to the arguments in the proof of Lemma,  $\dot{L}$  in (58) can be written as

$$\begin{aligned} \dot{L} &\leq -\rho_v \|\mathbf{x}\|^2 \quad \text{for } \lambda_{v2} \|\mathbf{x}_v(0)\|^2 \\ &< \lambda_{v1} \left( \frac{\gamma\lambda_q - 2\vartheta + \|\dot{\mathbf{q}}_d\| - 3\|B_d\| - \mu}{2\vartheta} \right)^2 \end{aligned} \quad (59)$$

where  $\rho_v$  is a constant. Thus we obtain the gain condition of (32).

Following the same arguments in the proof of Lemma, we can show that  $\lim_{t \rightarrow \infty} \mathbf{x} = 0$ , which implies the result given in Theorem 1.  $\square$

#### APPENDIX D PROOF OF THEOREM 2

In this case the Lyapunov function candidate (51) is modified as

$$L(t) = L_a(t) + \bar{L}_m(t) \quad (60)$$

where  $L_a(t)$  is defined in (42) and

$$\bar{L}_m(t) \triangleq \frac{1}{2} \tilde{\mathbf{I}}^T L_s \tilde{\mathbf{I}} + \frac{\frac{1}{2} \sum_{i=1}^3 (\bar{\delta}_i - \hat{\delta}_i)^2}{\eta_i}$$

where  $\bar{\delta}_1 = \delta_1$ ,  $\bar{\delta}_2 = \delta_2$ , and  $\bar{\delta}_3 = (\delta_3 + \zeta_2)$ ,  $\delta_i$  are defined in (26),  $\zeta_2$  is defined in (64), and  $\hat{\delta}_i$  are the estimates of  $\bar{\delta}_i$ . Given (60), one has

$$\lambda_{v1} \|\mathbf{x}_m\|^2 \leq V \leq \lambda_{v2} \|\mathbf{x}_m\|^2 \quad (61)$$

where  $\mathbf{x}_m^T \triangleq [\mathbf{x}^T \tilde{\alpha}_{ak}^T \tilde{\mathbf{I}}^T (\bar{\delta}_1 - \hat{\delta}_1), (\bar{\delta}_2 - \hat{\delta}_2), (\bar{\delta}_3 - \hat{\delta}_3)]$ ;  $\lambda_1$  and  $\lambda_2$  are defined in (52).

The time derivative of the first term  $L_a(t)$  in (60) is unchanged. Due to the change of the control  $\mathbf{V}$ , the derivative of  $\bar{L}_m(t)$  becomes

$$\begin{aligned} \dot{\bar{L}}_m = & -\tilde{\mathbf{I}}^T [L_s(\dot{\tilde{\mathbf{I}}}_m + \dot{\tilde{\mathbf{I}}}_f) + R_s \tilde{\mathbf{I}} + \mathbf{F}(\theta) K_e \dot{\hat{\mathbf{q}}}] \\ & - \mathbf{V} + R_s \mathbf{I}_d + \mathbf{F}(\theta) K_e \dot{\hat{\mathbf{q}}}_d \\ & + \frac{\sum_{i=1}^3 (\bar{\delta}_i - \hat{\delta}_i)(-\dot{\hat{\delta}}_i)}{\eta_i} \end{aligned} \quad (62)$$

where  $\mathbf{I}_f = [\mathcal{I}_{f1}^T, \dots, \mathcal{I}_{fn}^T]^T$ ,  $\mathcal{I}_{fi} \triangleq [\ell_{1i}^f, \ell_{2i}^f, \ell_{3i}^f]^T$ ,  $\ell_{ki}^f \triangleq u_{fi} h_{ki}(\theta_i)$ ,  $k = 1, 2, 3$ ,  $i = 1, \dots, n$ .

Since the compact form of  $\mathbf{I}_f$  can be expressed as  $\mathbf{I}_f = \mathbf{H}(\theta) \mathbf{u}_f$ , where  $H_i(\theta_i) \triangleq [h_{1i}, h_{2i}, h_{3i}]^T$ ,

$$\mathbf{H}(\theta) \triangleq \begin{bmatrix} H_1(\theta_1) & 0 & \dots & 0 & 0 \\ 0 & H_2(\theta_2) & \dots & 0 & 0 \\ \vdots & \vdots & \ddots & \vdots & \vdots \\ 0 & 0 & \dots & 0 & H_n(\theta_n) \end{bmatrix}$$

when  $\gamma \geq \max\{1, \kappa\}$ , one can write

$$\begin{aligned} -\tilde{\mathbf{I}}^T L_s \dot{\tilde{\mathbf{I}}}_f = & -\tilde{\mathbf{I}}^T L_s [\dot{\mathbf{H}} \mathbf{u}_f + \mathbf{H} \dot{\mathbf{u}}_f] \\ = & -\tilde{\mathbf{I}}^T L_s [(\dot{\mathbf{H}} \Phi_a + \mathbf{H} \dot{\Phi}_a) \hat{\alpha}_{ak} + \mathbf{H} \Phi_a \dot{\hat{\alpha}}_{ak}] \\ \leq & \alpha_l \|\tilde{\mathbf{I}}\| \|(\dot{\mathbf{H}} \Phi_a + \mathbf{H} \dot{\Phi}_a)\| \|\hat{\alpha}_{ak}\| \\ & + \|\mathbf{H} \Phi_a\| \|\dot{\hat{\alpha}}_{ak}\| \\ \leq & \alpha_l \|\tilde{\mathbf{I}}\| \|(\dot{\mathbf{H}} \Phi_a + \mathbf{H} \dot{\Phi}_a)\| \|\hat{\alpha}_{ak}\| \\ & + 3\sigma \|\Phi_a\|^2 \|\mathbf{H}\| \|\mathbf{x}\| \end{aligned} \quad (63)$$

where  $\alpha_l \triangleq \|L_s\|$  and (16) and (17) have been used.

Since  $\mathbf{H}$  is known, for simplicity of derivation, we assume here that  $\|\mathbf{H}\|$  can be bounded by a constant. If this is not the case, we can arrive at the same conclusion along a similar line of derivation. Recall that  $\dot{\hat{\mathbf{q}}}_d$ ,  $\ddot{\hat{\mathbf{q}}}_d$ , and  $\mathbf{q}_d^{(3)}$  are uniformly bounded, one can write

$$\begin{aligned} \|\mathbf{H}(\theta)\| & \leq \rho_1 \\ \|\Phi_a\| & \leq \rho_2 \\ \|(\dot{\mathbf{H}} \Phi_a + \mathbf{H} \dot{\Phi}_a)\| & \leq \varrho \|\dot{\hat{\mathbf{q}}}\| \end{aligned}$$

where  $\rho_1$ ,  $\rho_2$ , and  $\varrho$  are constants. Thus, the equation (63) becomes

$$\begin{aligned} -\tilde{\mathbf{I}}^T L_s \dot{\tilde{\mathbf{I}}}_f \leq & \alpha_l \varrho \|\tilde{\mathbf{I}}\| \|\dot{\hat{\mathbf{q}}}\| \|\hat{\alpha}_{ak}\| + 3\alpha_l \sigma \rho_1 \rho_2^2 \|\tilde{\mathbf{I}}\| \|\mathbf{x}\| \\ \leq & \alpha_l \varrho \|\tilde{\mathbf{I}}\| (\|\dot{\hat{\mathbf{q}}}\| + \|\ddot{\hat{\mathbf{q}}}_d\|) \|\hat{\alpha}_{ak}\| + 3\alpha_l \sigma \rho_1 \rho_2^2 \|\tilde{\mathbf{I}}\| \|\mathbf{x}\| \\ = & \alpha_l \varrho \|\tilde{\mathbf{I}}\| (\|\dot{\hat{\mathbf{q}}}\| + \|\mathbf{F}^T \mathbf{H}\| \|\dot{\hat{\mathbf{q}}}_d\|) \|\hat{\alpha}_{ak}\| \\ & + 3\alpha_l \sigma \rho_1 \rho_2^2 \|\tilde{\mathbf{I}}\| \|\mathbf{x}\| \\ \leq & \zeta_1 \|\tilde{\mathbf{I}}\| \|\mathbf{x}\| + \zeta_2 \|\mathbf{F}\| \|\dot{\hat{\mathbf{q}}}_d\| \|\tilde{\mathbf{I}}\| \end{aligned} \quad (64)$$

where  $\zeta_1 \triangleq (\alpha_l \varrho \|\hat{\alpha}_{ak}\| + 3\alpha_l \sigma \rho_1 \rho_2^2)$  and  $\zeta_2 \triangleq \alpha_l \varrho \rho_1 \|\hat{\alpha}_{ak}\|$ . It should be noted that in the above derivation we have used the relation  $\|\mathbf{F}^T \mathbf{H}\| = 1$ , which can easily be verified by using (23).

Substituting  $\mathbf{V}$  in (62) by the control law (35) and noticing (26) and (64), one obtains

$$\begin{aligned} \dot{\bar{L}}_m \leq & -\tilde{\mathbf{I}}^T R_s \tilde{\mathbf{I}} - \tilde{\mathbf{I}}^T \mathbf{F} K_e \dot{\hat{\mathbf{q}}} - \tilde{\mathbf{I}}^T L_s \dot{\tilde{\mathbf{I}}}_f + (\delta_1 \|\dot{\tilde{\mathbf{I}}}_m\| \|\tilde{\mathbf{I}}\| \\ & + \delta_2 \|\mathbf{I}_d\| \|\tilde{\mathbf{I}}\| + \delta_3 \|\mathbf{F}\| \|\dot{\hat{\mathbf{q}}}_d\| \|\tilde{\mathbf{I}}\|) \\ & - (\delta_1 \|\dot{\tilde{\mathbf{I}}}_m\| \|\tilde{\mathbf{I}}\| + \delta_2 \|\mathbf{I}_d\| \|\tilde{\mathbf{I}}\| + \delta_3 \|\mathbf{F}\| \|\dot{\hat{\mathbf{q}}}_d\| \|\tilde{\mathbf{I}}\|) \\ & + \frac{\sum_{i=1}^3 (\bar{\delta}_i - \hat{\delta}_i)(-\dot{\hat{\delta}}_i)}{\eta_i} \\ \leq & -\tilde{\mathbf{I}}^T R_s \tilde{\mathbf{I}} - \tilde{\mathbf{I}}^T \mathbf{F} K_e \dot{\hat{\mathbf{q}}} + \zeta_1 \|\tilde{\mathbf{I}}\| \|\mathbf{x}\| \\ \leq & -\tilde{\mathbf{I}}^T R_s \tilde{\mathbf{I}} + (\zeta_1 + \alpha_k) \|\mathbf{x}\| \|\tilde{\mathbf{I}}\|. \end{aligned} \quad (65)$$

Based on (55) and (65),  $\dot{L}$  can be expressed as

$$\begin{aligned} \dot{L} \leq & -(\gamma \lambda_q - 3\|B_d\| - 2\vartheta \|\dot{\hat{\mathbf{q}}}\|) \|\mathbf{x}\|^2 + \beta_1 \|\mathbf{x}\| \|\tilde{\mathbf{I}}\| - \tilde{\mathbf{I}}^T R_s \tilde{\mathbf{I}} \\ \leq & -(\gamma \lambda_q - 3\|B_d\| - 2\vartheta \|\dot{\hat{\mathbf{q}}}\| - \mu_1) \|\mathbf{x}\|^2 \\ & - \lambda_r (\|\tilde{\mathbf{I}}\| - \nu_1 \|\mathbf{x}\|)^2 \\ \leq & -(\gamma \lambda_q - 3\|B_d\| - 2\vartheta \|\dot{\hat{\mathbf{q}}}\| - \mu_1) \|\mathbf{x}\|^2 \end{aligned} \quad (66)$$

where

$$\begin{aligned} \beta_1 & \triangleq (3\alpha_f + \zeta_1 + \alpha_k) \\ \mu_1 & \triangleq \frac{\beta_1^2}{4\lambda_r} \\ \nu_1 & \triangleq \frac{\beta_1}{2\lambda_r} \end{aligned}$$

and

$$\lambda_r \triangleq \inf \frac{\tilde{\mathbf{I}}^T R_s \tilde{\mathbf{I}}}{\|\tilde{\mathbf{I}}\|^2}$$

Similar to the arguments in the proof of Lemma,  $\dot{L}$  in (66) can be written as

$$\begin{aligned} \dot{L} \leq & -\rho_m \|\mathbf{x}\|^2 \quad \text{for } \lambda_{v2} \|\mathbf{x}_m(0)\|^2 \\ < & \lambda_{v1} \left( \frac{\gamma \lambda_q - 2\vartheta + \|\dot{\hat{\mathbf{q}}}_d\| - 3\|B_d\| - \mu_1}{2\vartheta} \right)^2 \end{aligned} \quad (67)$$

where  $\rho_m$  is a constant. Thus we obtain the gain condition of (39).

Following the same arguments in the proof of Lemma, we can show that  $\lim_{t \rightarrow \infty} \mathbf{x} = 0$ , which implies the result given in Theorem 2.  $\square$

## REFERENCES

- [1] H. Asada and K. Youcef-Toumi, *Direct Drive Robots: Theory and Practice*. Cambridge, MA: MIT Press, 1987.
- [2] R. W. Beekmann and K. Y. Lee, "Nonlinear robotic control including drive motor interactions," in *Proc. Amer. Contr. Conf.*, Atlanta, 1988, pp. 1333-1338.
- [3] D. M. Dawson, J. J. Carrol, and M. Schneider, "Integrator backstepping control of a brush DC motor turning a robotic load," *IEEE Trans. Contr. Syst. Tech.*, vol. 2, pp. 233-244, 1994.
- [4] D. M. Dawson, Z. Qu, and J. J. Carrol, "Tracking control of rigid-link electrically-driven robot manipulator," *Int. J. Contr.*, vol. 56, pp. 911-1006, 1992.
- [5] M. C. Good, L. M. Sweet, and K. L. Strobel, "Dynamic models for control system design of integrated robot and drive systems," *J. Dyn. Syst., Meas., and Contr.*, vol. 107, pp. 53-59, 1985.
- [6] R. Guenther and L. Hsu, "Variable structure adaptive cascade control of rigid-link electrically-driven robot manipulators," in *Proc. IEEE Conf. on Decision and Contr.*, 1993.
- [7] J. Hu, D. M. Dawson, and J. J. Carroll, "An adaptive integrator backstepping tracking controller for brushless DC motor/robotic load," in *Proc. Amer. Contr. Conf.*, 1994, pp. 1401-1405.
- [8] I.-J. Ha and C.-I. Kang, "Explicit characterization of all feedback-linearizing controllers for a general type brushless DC motor," *IEEE Trans. Automat. Contr.*, vol. 39, pp. 673-677, 1994.
- [9] H. Hashimoto *et al.*, "Brushless servo motor control using variable structure approach," *IEEE Trans. Indust. Applicat.*, vol. 24, pp. 160-170, 1988.
- [10] N. Hemati and M. Leu, "A complete model characterization of brushless DC motors," *IEEE Trans. Indust. Applicat.*, vol. 28, pp. 172-180, 1992.
- [11] N. Hemati, J. Thorp, and M. Leu, "Robust nonlinear control of brushless DC motors for direct-drive robotic applications," *IEEE Trans. Indust. Elec.*, vol. 37, pp. 498-501, 1990.
- [12] P. V. Kokotovic, "The joy of feedback: Nonlinear and adaptive," *IEEE Contr. Syst. Mag.*, vol. 12, no. 3, pp. 7-17, 1992.
- [13] P. Pillay and R. Krishnan, "Modeling, simulation, and analysis of permanent-magnet motor drivers, Part 2: The brushless DC motor drive," *IEEE Trans. Indust. Applicat.*, vol. 25, pp. 274-279, 1989.
- [14] H. Sira-Ramirez, "On the dynamical sliding mode control of nonlinear systems," *Int. J. Contr.*, vol. 57, pp. 1039-1061, 1993.
- [15] J. J. E. Slotine and W. Li, "Adaptive manipulator control: A case study," *IEEE Trans. Automat. Contr.*, vol. 33, pp. 995-1003, 1988.
- [16] C.-Y. Su, T. P. Leung, and Y. Stepanenko, "Real-time implementation of regressor based sliding mode control scheme for robot manipulators," *IEEE Trans. Indust. Electron.*, vol. 40, pp. 71-79, 1993.
- [17] C.-Y. Su and Y. Stepanenko, "On the robust control of robot manipulators including actuator dynamics," *J. Robotic Syst.*, vol. 13, pp. 1-10, 1996.
- [18] T. J. Tarn, A. K. Bejczy, X. Yun, and Z. Li, "Effect of motor dynamics on nonlinear feedback robot arm control," *IEEE Trans. Robot. Automat.*, vol. 7, pp. 114-122, 1991.
- [19] D. Taylor, "Composite control of direct-drive robots," in *Proc. 28th Conf. on Decision and Contr.*, 1989, pp. 1670-1675.
- [20] V. I. Utkin, *Sliding Modes and Their Applications*. Moscow: Mir, 1978.
- [21] J. Yuan and Y. Stepanenko, "Composite adaptive control of flexible joint robots," *Automatica*, vol. 29, pp. 609-619, 1993.
- [22] ———, "Robust control of robotic manipulator without joint velocity feedback," *Int. J. Robust and Nonlinear Contr.*, vol. 1, pp. 203-213, 1991.



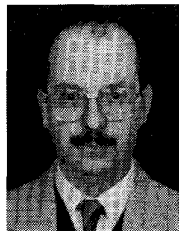
**Chun-Yi Su** (M'93) was born in Xining, China, in 1962. He received the B.E. degree in control engineering from Shaanxi Institute of Mechanical Engineering (now Xi'an University of Technology) in 1982, the M.S. and Ph.D. degrees in control engineering from South China University of Technology, China, in 1987 and 1990, respectively (He jointly received the Ph.D. degree from Hong Kong Polytechnic University, Hong Kong).

He has been with the Department of Mechanical Engineering, University of Victoria, Canada, since 1991. His current research interests are in the area of control of nonlinear feedback systems, and include applications to control of mechanical systems. Dr. Su received an Outstanding Paper Award from the Acta Automatica Sinica in 1992.



**Yury Stepanenko** received the Ph.D. degree for his work on the analysis of nonlinear servosystems from the Moscow Institute of Machine Science, Moscow, Russia, in 1964. He received the D.Sc. degree in robotic research from the same university in 1971.

He is now a Professor in the Department of Mechanical Engineering at the University of Victoria, British Columbia, and Director of the Adaptive Robotic Telesystems Laboratory. He has been a Senior Researcher in the Moscow Institute of Machine Science, Professor and Chairman of the Department of Automatic Control at the Institute of Machine-Tool Engineering, Moscow, and Senior Consultant at the Iskra Corporation, Slovenia. He is the author and co-author of more than 120 scientific papers and one monograph, "Dynamics of Spatial Mechanisms." He holds ten patents. His research interests are in dynamics and control of nonlinear systems and robotics.



**Sadik Dost** received the B.Sc. and M.Sc. degrees from Karadeniz Technical University, Turkey and the Ph.D. degree from Istanbul Technical University, Istanbul, Turkey.

He is a Professor of mechanical engineering and the founding Director of the Center for Advanced Materials and Related Technology, University of Victoria, Victoria, B.C., Canada. He has received several awards and certificates for outstanding engineering and research achievements. He currently serves on various advisory and editorial boards. He has published over 150 journal and conference papers, and book contributions. He has engaged in a fairly broad spectrum of research actively ranging from transport phenomena in various engineering applications to processing of piezoelectric and semiconductor materials for various applications in actuators, sensors, and optoelectronics. Piezoceramics for actuators and single crystal semiconductors of Si, GaAs, and GaInAs are among his current research interests.

Dr. Dost is a Fellow of CSME and EIC.